ISRN LUTMDN/TMHP—08/5138—SE
ISSN 0282-1990

Model Simplification and Observer Design of a Turbo Charged Engine

Christofer Sundström

Thesis for the Degree of Master of Science

Division of Combustion Engines
Department of Energy Sciences
Faculty of Engineering, LTH
Lund University
P.O. Box 118
SE-221 00 Lund
Sweden

Model Simplification and Observer Design of a Turbo Charged Engine

Master's thesis

performed in **Division of Combustion Engines**,
Department of Energy Sciences
at **Lund Institute of Technology**

by **Christofer Sundström**

ISRN LUTMDN/TMHP-08/5138-SE

Supervisor: **Associate Professor Lars Eriksson**
Linköpings Universitet
Ph.D. Student Johan Wahlström
Linköpings Universitet

Examiner: **Associate Professor Per Tunestål**
Lund Institute of Technology

Lund, February 5, 2008

Abstract

Tougher legislation and higher expectations on the comfort of the vehicles, forces the vehicle manufacturers to make progress. To manage the demands, it is crucial to correctly estimate the air mass-flow to the cylinders. To estimate the mass-flow, a mean value engine model (MVEM) could be used. Since the computational power in the controller system is limited, the original MVEM has to be modified. The purpose is to reduce the required sample frequency to run the model.

Firstly, some of the states in the original model are reduced and replaced by statical equations. The objective of this is to replace states that have fast dynamics with statical expressions. The reduction in sample frequency required to simulate the model is though less than expected.

Some equations in the original model are modified when large derivatives occur. By increasing the size of the regions where the modified equations are used, these large derivatives become smaller. Furthermore, a solver with high resolution for a part of the model, at the same time as a solver with lower sample frequency is used for the entire model, is implemented.

The reduction in computational effort using these modifications does not fulfill the required demands. Therefore, three different observers are implemented. They are based on the model for the throttle and the volumetric efficiency in the original MVEM, to estimate the air mass-flow to the cylinders. Since the observers do not model the entire engine, the signals from the sensors are always used. This is not preferable during transients. The sample frequency to achieve a stable model is though acceptable.

Keywords: MVEM, Turbocharged, SI-engine, Model reduction, Observer

Preface

This thesis is written for readers with good knowledge in spark ignited (SI)-engines. The readers are also expected to have knowledge about mean value engine modeling (MVEM), since only a short introduction to the MVEM used is found in the thesis. For the interested reader, Per Anderssons PhD thesis *Air Charge Estimation in Turbocharged Spark Ignition Engines* [1] is recommended. In Anderssons thesis, the MVEM, that this thesis work is based on, is developed and validated.

Acknowledgment

I would like to thank my supervisors Lars Eriksson and Johan Wahlström at vehicular system. They have always come up with new ideas and there have been several interesting discussions. Johan has done a tremendous job proof reading the report. Andreas Jerhammar at GM Powertrain has been helpful by e.g. presenting measure data. I have had many interesting and humorous discussions with Oskar Leufven. When Oskar haven't been able to help me when problems with the computer have occurred, Per Öberg has always been helpful. Finally I like to thank the rest of the group at vehicular systems for many interesting breaks in the lunch room.

Contents

Abstract **iii**

Preface and Acknowledgment **iv**

1 Introduction and Outline **1**
1.1 Introduction . . . 1
1.1.1 Mean value engine model . . . 1
1.1.2 Control volumes . . . 2
1.1.3 Restrictions . . . 2
1.2 Problem formulation . . . 4
1.3 Sample frequency and accuracy . . . 4
1.4 Outline . . . 5

2 Reduction of States **6**
2.1 Modified components . . . 6
2.1.1 Air filter . . . 6
2.1.2 Compressor . . . 7
2.1.3 Intercooler . . . 9
2.1.4 Intake manifold . . . 9
2.1.5 Exhaust manifold . . . 9
2.1.6 Exhaust system . . . 9
2.2 Reduction of one control volume . . . 10
2.2.1 Initial conditions . . . 10
2.2.2 Results from simulations . . . 11
2.3 Reduction of more than one control volume . . . 14

3 Change Linear Regions **15**
3.1 Components using linear regions . . . 15
3.2 Results . . . 15
3.2.1 Air-filter and compressor modified . . . 16
3.2.2 Air-filter, compressor and exhaust system modified . . . 16
3.2.3 Air-filter, compressor, intake manifold and exhaust system modified . . . 17
3.2.4 Air-filter, compressor, intake manifold, exhaust manifold and exhaust system modified . 17

4 Local Differential solver **18**
4.1 Solvers used . . . 18
4.1.1 Euler . . . 18
4.1.2 Euler using Richardsson extrapolation . . . 18
4.1.3 Euler using repeated Richardsson extrapolation . . . 18
4.2 Local solver for the Intercooler . . . 19
4.2.1 Different global solvers . . . 19
4.2.2 Different throttle angles . . . 19

5 Observer **20**
5.1 Volumetric efficiency 20
5.2 $\dot{p}_{im}$ integrated 21
5.3 $\dot{W}_{cyl}$ integrated 21
5.4 Basis for comparison 22
5.5 Results 22
5.5.1 Low pass filter 22
5.5.2 Different observers 22

6 Summary and Conclusions **26**

7 Future Work **27**

References **28**

Nomenclature **29**

Chapter 1

Introduction and Outline

1.1 Introduction

Turbocharged spark ignited engines are becoming more and more common in vehicles. Not only in powerful vehicles, but also in downsized engines where the objective is to reduce fuel consumption. There are many perspectives to take into consideration when designing the controller for the turbocharger and the engine in total. In order to decrease the development time for new vehicles in combination with cost savings, models are being more and more used in predevelopment phases.

Legal demands on emissions are being tougher on the vehicle manufactures. It is of highest importance that the air/fuel mixture is stoichiometric in an SI-engine, for the catalyst to operate efficient. To achieve this, the air massflow to the cylinders have to be predicted accurately. During transients this is a problem, since it takes some time for the sensors to react on the change. Therefore, it would be preferable to use a model that estimates the flow accurately, especially during changes in operating points.

There are two main ways to model an SI-engine. One way to go is to make a model that has high resolution and for example accounts for when in the cycle the combustion occurs. The disadvantage of this method is that it is needed to sample in the order of every crank angle degree of the engine. If the engine is running at 2000 rpm this results in that the sample frequency has to be about 12000 Hz. Even using a modern computer it will take considerable time to simulate a driving cycle that is a few minutes.

The other approach is to assume that there is a continuous flow of air and fuel to the cylinders, that are transformed into heat and torque. The advantage of doing this is that the sample frequency can be dramatically decreased and still result in a reasonably accurate model. This type of models are called mean value engine models (MVEM). The content of this thesis is to modify an already existing MVEM, developed and validated in [1]. The objective of the modification is to reduce the computational effort required to run the model. This is important to be able to run the model in real time on the vehicle, to estimate the air massflow to the cylinders. The computational power on the vehicle is limited and cannot handle the original MVEM.

1.1.1 Mean value engine model

The MVEM used in this thesis consists of several components, such as air-filter, intercooler and throttle. The advantage of modeling each component separately is that each component can be modified to fit a specific engine without replacing the structure of the model. A component consists of one generalized restriction and one control volume. The restrictions estimate the mass-flow through the component, mainly from the pressures and temperatures before and after the restriction. The control volumes calculate the pressure and temperature in the volume between two restrictions. These quantities are represented as states in the model.

There are six control volumes in the model, see figure 1.1, that result in 12 states. In addition, the speed of the turbo charger is a state, which results in that the model contains 13 states. The states are given in table 1.1.

The MVEM is a stiff model since there are both slow and fast dynamics in the system. As a consequence, to be able to simulate the model the sample frequency has to be reasonably high. To achieve a stable simulation using Euler as the solver for the differential equations, the sample frequency has to be approximately 500 Hz. The model is accurate and the error is less than 5 % in most operating points.

The usage of the model is twofold. One purpose is to simulate whole driving cycles instead of using a real engine. The other objective is to use the model for controlling the engine by estimating the mass-flows through

different components. The model is used in combination with sensors, that are more accurate than the model in steady state. During transients the sensors are not able to react fast enough to changes in mass-flow, pressure and temperature. In these cases the model is more accurate and should therefore be used to estimate the flows in the engine instead of the sensors. This leads to that it is of high interest to achieve a high accuracy in transients in the model.

Table 1.1: States used in the model in figure 1.1.

State	Description
p_{af}	Pressure after air-filter
T_{af}	Temperature after air-filter
p_{comp}	Pressure after compressor
T_{comp}	Temperature after compressor
p_{ic}	Pressure after intercooler
T_{ic}	Temperature after intercooler
p_{im}	Pressure in intake manifold
T_{im}	Temperature in intake manifold
p_{em}	Pressure in exhaust manifold
T_{em}	Temperature in exhaust manifold
p_{es}	Pressure after turbine
T_{es}	Temperature after turbine
ω_{TC}	speed of turbocharger

1.1.2 Control volumes

The pressure and temperature is modeled in the control volumes using mass and energy conservation in combination with the ideal gas law, as in equation 1.1. Rewriting the ideal gas law and then differentiate it with respect to time, the expression for $\frac{dp}{dt}$ is found in equation 1.2. The first term in the expression represents the difference in mass-flow in and out from the model and the second the impact of the pressure due to the change in temperature. The expression for $\frac{dT}{dt}$ is based on energy conservation and is given in equation 1.3.

$$m = \frac{pV}{RT} \tag{1.1}$$

$$\frac{dp}{dt} = \frac{RT}{V}\left(W_{in} - W_{out}\right) + \frac{mR}{V}\frac{dT}{dt} \tag{1.2}$$

$$\frac{dT}{dt} = \frac{1}{mc_v}\left(W_{in}c_v\left(T_{in} - T\right)\right) + \frac{1}{mc_v}\left(R\left(T_{in}W_{in} - TW_{out}\right) + \dot{Q}\right) \tag{1.3}$$

The assumptions made, modeling the control volumes with the equations above are the following:

- the fluid is a perfect gas
- constant temperature in the whole control volume
- immediate and complete mixture in the volume

1.1.3 Restrictions

Conventionally a restriction is a component that decreases the pressure. This is the case in e.g. the air-filter. In the MVEM, the compressor and the engine rather acts as pumps. All these blocks are called restrictions in this thesis. In the model there are two different assumptions for the restrictions used. In the air-filter, intercooler and exhaust system, the flow is assumed to be incompressible. The flows through the throttle and wastegate are assumed to be incompressible.

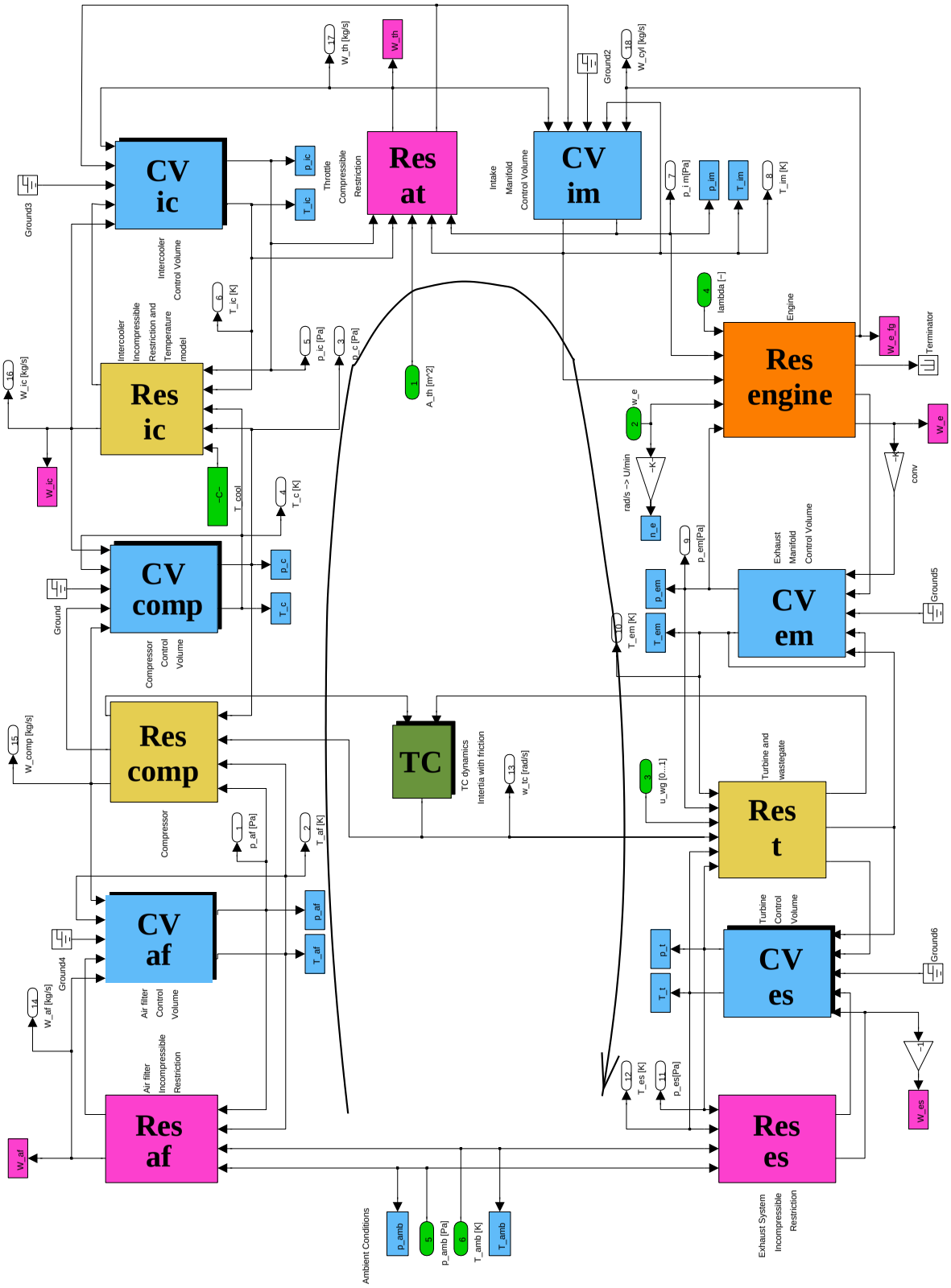

Figure 1.1: The original MVEM. The flow starts in the lower left corner and ends in the lower right corner after passing all components. The turbo charger shaft is seen in the middle, joining the compressor in the intake and the turbine in the exhaust parts of the model. In the figure *CV* is control volume and *Res* is restriction.

Incompressible restrictions

The components where the flow is assumed to be incompressible are also assumed to be isenthalpic [2]. This results in that the temperature remains the same in the actual component. The pressure drop for an incompressible flow can be described as in equation 1.4 and might be caused by e.g. wall friction or change in area of the pipe.

$$\Delta p_r = p_{us} - p_{ds} = H_r \frac{T_{us} W^2}{p_{us}} \tag{1.4}$$

From equation 1.4 the mass-flow can be expressed, see equation 1.5.

$$W = \sqrt{\frac{p_{us}}{H_r T_{us}}} \sqrt{p_{us} - p_{ds}} \tag{1.5}$$

The derivate of the mass-flow with respect to p_{us} gives $\frac{dW(p_{us})}{dp_{us}} \rightarrow -\infty$ when $\Delta p \rightarrow 0$. This could be troublesome for the solver of the model to handle. Therefore an alternative expression for the mass-flow, when the difference in pressure is small is used. The original expression is simply linearized. When the pressure is greater downstream than upstream the mass-flow will be negative, but the implemented model doesn't handle back-flows. Therefore the mass-flow is set to zero if that occurs.

The model for the intercooler uses the same basic equations as above, with the exception that the temperature is changed in the restriction.

Compressible restrictions

The assumption above that the fluid is incompressible is only valid when the speed of the fluid is less than approximately 30 % of the speed of sound [4]. In the model this may not be fulfilled for all operating points in the throttle and wastgate. Therefore the change in density of the fluid has to be considered. The equation for the mass-flow through the throttle can easily be generalized and is given in equation 2.14.

1.2 Problem formulation

The problems to be investigated during this thesis are:

- Decrease the required sample frequency to maximum 80 Hz from the original model that requires approximately 500 Hz. To solve the differential equations in the model, explicit Euler should be used.
- Investigate what properties influence the sample frequency the most.
- Achieve an acceptable accuracy in the model when the sample frequency is decreased. This is most important during transients. In steady state the sensors can be used instead of the model.

1.3 Sample frequency and accuracy

The objective with the modified models is to use them as observers in vehicles and are therefore dependent on data measured by sensors. The sensors have a limited sample frequency, that limits the step length in the model. In the report, the inverse to the step length is used as a measure of the stability of the model and is called sample frequency.

There are two different errors that could be used, either the absolute or relative error. The absolute error is to prefer if the emissions are of highest interest. This is due to that the catalyst can buffer a specific amount of oxygen. That results in that an error in the estimated air mass-flow, not is a problem as long as the catalyst not is full or empty of oxygen. The relative error is to prefer if the vehicle performance is the most important task to optimize. The reason for this is that the driver can feel jerks, if the engine for example is run lean. This is more dependent on λ, which is a relative quantity, than on the size of the error in the estimation of the mass-flow. In this work the relative error is used to compare different configurations of the model.

When simulations are carried out, it is of highest interest to investigate at what sample frequency the model gives an acceptable accuracy. To be able to compare different models with each other, five different measures of the error in the simulations are introduced and explained below. Instead of collecting measurement data from a running engine, the original model is assumed to generate the true values.

$e_{I,m}$ This error represents the difference between the original and modified models. Both models are solved using an implicit solver with variable step length. The signals used to calculate the error are the mass-flow to the cylinders,W_{cyl}, and the error induced is due to model simplifications. The I in the index represents that the results from the simulations are only studied in a certain range. The steps in throttle angle occurs after 10 and 18 seconds, see figure 2.2. Since it is of highest interest that the model is accurate during transients the difference between the models are only studied from the steps occur till 0.2 seconds after the steps. The difference is integrated and normalized with the air mass-flow to the cylinder in the original model, see equation 1.6. In the thesis the error is presented in percent.

$$e_I = \frac{\int_t^{t+0.2} |W_{org} - W_{mod}|\, dt}{\int_t^{t+0.2} W_{org} dt} \tag{1.6}$$

$e_{I,s}$ This error is a measure of the error induced by the solver. The solver that should be used in the final version is explicit Euler. Therefore the amplitude of $e_{I,s}$ is dependent on the sample frequency. The models compared are the ideal solved modified model and the modified model solved with Euler. Since there is no algebraic way to solve the model, a variable step implicit solver with high accuracy is used instead.

$e_{I,t}$ The ideal solution from the original model is compared to the modified model solved by explicit Euler, and results in the total error. The time the error is integrated is the same as for the previous errors.

$\overline{e_s}$ The error is calculated in the same way as $e_{I,s}$. The only difference is that $\overline{e_s}$ is calculated over the whole driving cycle, not only during transients.

$\tilde{e}_t$ The difference between the original model and the modified model solved by explicit Euler is calculated in every sample. $\tilde{e}_t$ gives the maximum difference over the whole driving cycle between the two models.

The demands on the model is given below. If one or more of the conditions not are fulfilled, the model is not accurate enough. Most of the time it helps to increase the sample frequency in order to get a more accurate simulation. For the different models used, a sample frequency is presented for the model. To find at what sample frequency the simulation fulfills the demands, simulations with different frequencies are carried out. If the demands are fulfilled, the sample frequency are decreased, otherwise increased. This is done in steps of 10 Hz.

- $e_{I,t} < 3\%$
- $\overline{e_s} < 1\%$
- $\tilde{e}_t < 8\%$

1.4 Outline

Several approaches for increasing the stability in the model are investigated. In chapter 2, states in the original MVEM are removed. Different configurations of the model is implemented and analyzed. For the model configurations with most potential, the linear regions impact on the stability in the model are controlled. This is done in chapter 3. A local solver for the states in the intercooler are implemented in chapter 4, since there is fast dynamics in that component. In chapter 5, three different observers are developed and evaluated. Finally, conclusions and future work are presented in chapters 6 and 7.

Chapter 2

Reduction of States

In this chapter the number of states in the model is reduced. The objective of this is to reduce the states with fastest dynamics in order to decrease the largest eigenvalues of the system. This leads to that a lower sample frequency is required to achieve a stable and accurate simulation, accordingly to the inequality in equation 2.1, that has to be fulfilled to guarantee a stable simulation. In the equation, h is the step size and λ the eigenvalues of the system.

$$|1 + h\lambda| < 1 \tag{2.1}$$

2.1 Modified components

In this section modified components will be designed. The purpose of this is to later be able to use one or many of the modified components in the MVEM.

To be able to remove a state, or even a whole control volume, the dynamics of that component is assumed to be negligible for the outputs of the model. This means that $\frac{dT}{dt} = 0$ and $\frac{dp}{dt} = 0$.

The general expression for the change in pressure in a control volume is given in equation 2.2. By assuming that the temperature gradient inside the control volume is zero and that there is no dynamics in the pressure, the air mass-flows must be equal, see equation 2.3. The mass-flows are dependent on the pressure in the control volume and thereby a static expression for the pressure in the actual component could be found.

$$\frac{dp}{dt} = \frac{R_a T_{up}}{V_{CV}} \left(W_{in} - W_{out}\right) + \frac{m_{CV} R_a}{V_{CV}} \underbrace{\frac{dT_{CV}}{dt}}_{=0} = 0 \tag{2.2}$$

$$W_{out} = W_{in} \tag{2.3}$$

Using equation 1.3 and assuming no dynamics in the temperature, the mass-flows in and out from the control volume are equal and that $\dot{Q} = 0$, the temperature has to be unchanged in the actual control volume.

2.1.1 Air filter

The control volume of the air filter is removed and thereby its states, p_{af} and T_{af}. The temperature out of the air filter is assumed to be ambient and the expression for the pressure is derived using equation 2.3. The mass-flow through the air filter, W_{af}, and the flow through the compressor, W_{comp}, are in this case assumed to be equal, see equations 2.4 and 2.5. K_1 and K_2 are parameters of the compressor used. From the mass-flows an expression for the pressure in the air filter, p_{af}, is determined, see equation 2.9. In the original model there is a linear region in the expression of the air mass-flow through the air filter. This is to avoid getting infinitely large numbers when the flow is differentiated in operating points where the pressure after the air filter is close to the ambient pressure. When this region is implemented in the modified component the stability of the model decreased and therefore only the equation for the regular region is used. This region is the physical description of the mass-flow and should thereby result in higher accuracy in the model.

To be able to find an expression for p_{af}, the following assumption has to be made. p_{af} is part of the pressure ratio, Π_{comp} (see equation 2.6), that is used in the expression for W_{comp}. Since Π_{comp} is raised with an exponent

in equation 2.5, the equations are difficult to solve. Instead the pressure in the air-filter from previous sample is used in Π_{comp} and can thereby be seen as a constant in the equations.

$$W_{af} = \begin{cases} \sqrt{p_{amb}\frac{p_{amb}-p_{af}}{H_{af}T_{af}}} & p_{amb} - p_{af} > p_{af,lin} \\ \sqrt{\frac{p_{amb}}{H_{af}T_{amb}}}\frac{p_{amb}-p_{af}}{\sqrt{p_{af,lin}}} & 0 \leq p_{amb} - p_{af} \leq p_{af,lin} \\ 0 & p_{amb} - p_{af} < 0 \end{cases} \tag{2.4}$$

$$W_{comp} = \frac{p_{af}}{R_a T_{af}}\frac{\pi}{4}D_{comp}^2 U_{comp}\sqrt{\frac{1 - \min\left(K_1\left(c_{pa}T_{af}\frac{-1+\Pi_{comp}^{\frac{\gamma_a-1}{\gamma_a}}}{\frac{1}{2}U_{comp}^2}\right)^2, 1\right)}{K_2}} \tag{2.5}$$

$$\Pi_{comp} = \frac{p_{comp}}{p_{af}} \tag{2.6}$$

2.1.2 Compressor

The compressor has slow dynamics due to the inertia of the turbocharger. This results in that it takes time for the turbocharger to change speed when the operating point of the engine is changed. Since this dynamics mainly is due to the inertia of the turbocharger, a modified version of the compressor restriction and its control volume is implemented, where p_{comp} and T_{comp} are removed. This only leads to a small change in the compressor dynamics. The modified component ignores the dynamics in the volume between the compressor and the intercooler. The mass-flows that are used in equation 2.3 are W_{comp} and the flow through the intercooler, W_{ic}, given in equation 2.7. The expression for the pressure after the compressor is determined to be as in equation 2.10 and the expression for the linear region is given in equation 2.8.

$$W_{ic} = \begin{cases} \sqrt{p_{comp}\frac{p_{comp}-p_{ic}}{H_{ic}T_{comp}}} & p_{comp} - p_{ic} > p_{ic,lin} \\ \sqrt{\frac{p_{comp}}{H_{ic}T_{comp}}}\frac{p_{comp}-p_{ic}}{\sqrt{p_{ic,lin}}} & 0 \leq p_{comp} - p_{ic} \leq p_{ic,lin} \\ 0 & p_{comp} - p_{ic} < 0 \end{cases} \tag{2.7}$$

$$p_{comp,Lin} = p_{ic} + \frac{D_C^3\omega_{TC}p_{af}\sqrt{p_{comp,lin}}\pi\sqrt{\frac{1-\min\left(1, \frac{64c_{pa}^2K_1\left(-1+\Pi_{comp}^{\frac{\gamma-1}{\gamma}}\right)^2}{D_c^4\omega_{TC}^4}\right)}{K_2}}}{8K_2R_a^2T_{af}^2\sqrt{\frac{p_{comp,old}}{H_{ic}T_{comp}}}} \tag{2.8}$$

$$p_{af} = \frac{4K_2 p_{amb}^2 R_a^2 T_{af}}{2K_2 p_{amb} R_a^2 T_{af} + \sqrt{K_2 p_{amb}^2 T_{af} \left(4K_2 R_a^2 T_{af} - D_c^4 H_{af} \pi^2 \left(-1 + \min\left(1, \frac{4c_{pa}^2 K_1 T_{af} \left(-1+\Pi_{comp}^{\frac{-1+\gamma}{\gamma}}\right)^2}{U_{comp}}\right)\right) U_{comp}\right)} \tag{2.9}$$

$$p_{comp} = \frac{p_{ic}}{2} + \frac{\sqrt{K_2 R_a^2 T_{af}^2 \left(16K_2 p_{ic}^2 R_a^2 T_{af}^2 + D_C^6 H_{ic} \omega_{TC}^2 p_{af}^2 \pi^2 T_{comp} - D_C^6 H_{ic} \omega_{TC}^2 p_{af}^2 \pi^2 T_{comp} \cdot \min\left(1, \frac{64c_{pa}^2 K_1 \left(-1+\Pi comp^{\frac{\gamma-1}{\gamma}}\right)^2 T_{af}}{D_c^4 \omega_{TC}^4}\right)\right)}}{8K_2 R_a^2 T_{af}^2} \tag{2.10}$$

$$p_{ic} = \frac{1}{2\left(p_{comp} R_a T_{ic} + A_{eff}^2 H_{ic} p_{im} T_{comp} x_1\right)} \left[p_{comp}^2 R_a T_{ic} + A_{eff}^2 H_{ic} p_{im} T_{comp} \left(x_1 - x_2\right) + \sqrt{\left(p_{comp}^2 R_a T_{ic} + A_{eff}^2 H_{ic} p_{im}^2 T_{comp} \left(x_1 - x_2\right)\right) + 4A_{eff}^2 H_{ic} p_{im}^3 T_{comp} \left(p_{comp} R_a T_{ic} + A_{eff}^2 H_{ic} p_{im} T_{comp} x_1\right) x_2}\right] \tag{2.11}$$

$$p_{ic,Lin} = \frac{1}{2A_{eff}^2 H_{ic} \Pi_{lin} T_{comp} \left(x_1 + \Pi_{lin} x_2\right)} \left[p_{comp} \left(-1 + \Pi_{lin}\right) R_a T_{ic} + 2A_{eff}^2 H_{ic} \Pi_{lin} p_{im} T_{comp} \left(x_1 + \Pi_{lin} x_2\right) + \sqrt{p_{comp} \left(\left(-1 + \Pi_{lin}\right) R_a T_{ic} \left(4A_{eff}^2 H_{ic} \Pi_{lin} p_{im} T_{comp} \left(x_1 + \Pi_{lin}\right) + \left(\left(-1 + \Pi_{lin}\right) R_a T_{ic} - 4A_{eff}^2 H_{ic} \Pi_{lin} T_{comp} \left(x_1 + \Pi_{lin}\right)\right)\right)\right)}\right] \tag{2.12}$$

$$p_{ic,Crit} = \frac{2p_{comp}^2 R_a T_{ic}}{p_{comp} R_a T_{ic} - \sqrt{p_{comp}^2 R_a T_{ic} \left(R_a T_{ic} - 4A_{eff}^2 H_{ic} \left(-1 + \Pi_{crit}\right) \Pi_{crit} T_{comp} \left(x_1 \Pi_{crit} x_2\right)\right)}} \tag{2.13}$$

2.1.3 Intercooler

Two modified versions of the intercooler are also implemented. In one of the modified components, the temperature state is reduced. In the alternative model both p_{ic} and T_{ic} are reduced. Most likely, at least the pressure of either the compressor or the intercooler control volumes has to be unchanged. This is to catch the dynamics between the compressor and the throttle. Though the dynamics in temperature might be removed in both the intercooler and the compressor at the same time. The pressure after the intercooler, p_{ic}, was calculated accordingly to equation 2.11. The mass-flows used to derive the expression for p_{ic} are the throttle, W_{at} (see equation 2.14), and W_{ic}. Furthermore an assumption has to be made in the expression for W_{at} in order to solve p_{ic}. In the calculation the Ψ-function, see equation 2.15 and 2.16, p_{ic} is part of Π and is difficult to solve. Therefore, a simplification of the Ψ-function is made in equation 2.17 and the coefficients x_1 and x_2, are estimated with the least square method.

In the original model there are three different regions in the Ψ-function implemented. The purpose of the linear region is to avoid large derivatives in the model. The Ψ-function is plotted in figure 2.1. The region in the middle of the curve is used to calculate p_{ic}. In equations 2.12 and 2.13 the pressures in the other two regions of the intercooler are given.

$$W_{at} = \frac{p_{ic}}{\sqrt{R_a T_{ic}}} \Psi\left(\Pi\right) A_{eff}\left(\alpha\right) \tag{2.14}$$

$$\Psi(\Pi) = \begin{cases} 1 & 0 < \Pi \leq \left(\frac{2}{\gamma+1}\right)^{\frac{\gamma}{\gamma-1}} \\ \Psi^*(\Pi) & \left(\frac{2}{\gamma+1}\right)^{\frac{\gamma}{\gamma-1}} < \Pi \leq \Pi_{lin} \\ \Psi^*(\Pi)\frac{\Pi-1}{\Pi_{lin}-1} & \Pi_{lin} < \Pi \leq 1 \end{cases} \tag{2.15}$$

$$\Psi^*(\Pi) = \sqrt{\frac{2\gamma}{\gamma-1}\left(\Pi^{\frac{2}{\gamma}} - \Pi^{\frac{\gamma+1}{\gamma}}\right)} \tag{2.16}$$

$$\Psi^*(\Pi) \approx \sqrt{\left(x_1 + x_2\Pi\right)\left(1-\Pi\right)} \tag{2.17}$$

$$\Pi = \frac{p_{im}}{p_{ic}} \tag{2.18}$$

2.1.4 Intake manifold

The temperature state, T_{im}, is replaced by the input signal to the original control volume. The pressure is still a state since the dynamics in the flow around the throttle is significant at some operating points. It is important to get the mass-flow to the cylinders as accurate as possible since the amount of injected fuel is dependent on the air mass-flow.

2.1.5 Exhaust manifold

The modified version of this component has no temperature dynamics. The dynamics in pressure is though always implemented in the model.

2.1.6 Exhaust system

The control volume is replaced by static equations for p_{es} and T_{es} in the modified version of this component. The expression used for the pressure after the turbine, p_{es}, is presented in equation 2.22. The mass-flows used are given in equations 2.19-2.21. The mass-flow through the exhaust system, W_{es}, is assumed to be equal to the sum of the flows through the turbine W_t, and the wastegate, W_{wg}. In the model W_t and W_{wg} is calculated and therefore these variables are used in the expression for p_{es}. The advantage of this is that the approximation made in the air-filter using the old p_{comp} is not needed in this component.

$$W_t = \begin{cases} \frac{p_{em}}{\sqrt{T_{em}}} k_1 \sqrt{1-\Pi_t^{k_2}} & \Pi_t^{k_2} \leq 1 \\ 0 & otherwise \end{cases} \tag{2.19}$$

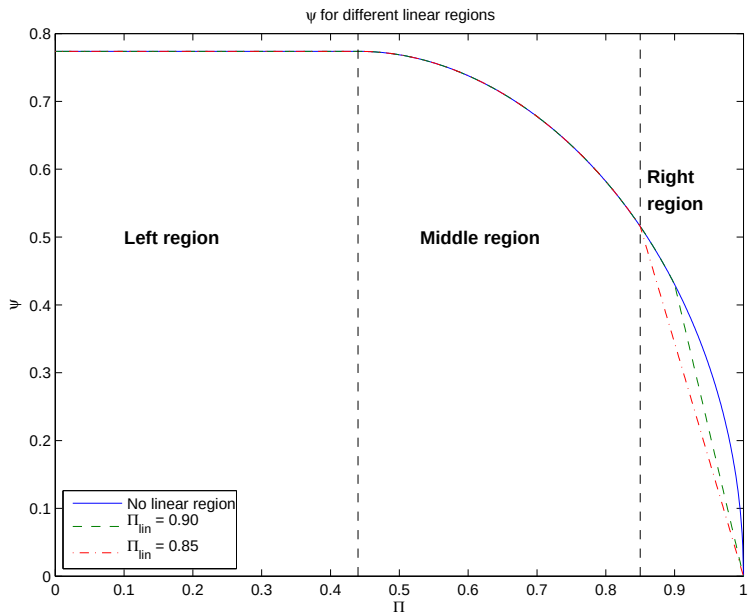

Figure 2.1: The Ψ-function as a function of Π. The region to the left is the critical region, in the middle the regular and the region close to 1 is the linear region for two of the curves. Π_{lin} is 0.85 respectively 0.90 in the cases where the linear region is used.

$$W_{wg} = \frac{p_{em}}{\sqrt{R_{eg}T_{em}}}\Psi_{em(\Pi_t)A_{eff,wg}}\left(u_{wg}\right) \tag{2.20}$$

$$W_{es} = \begin{cases} \sqrt{p_{es}\frac{p_{es}-p_{amb}}{H_{af}T_{es}}} & p_{es}-p_{amb} > p_{es,lin} \\ \sqrt{\frac{p_{es}}{H_{af}T_{es}}}\frac{p_{es}-p_{amb}}{\sqrt{p_{es,lin}}} & 0 \leq p_{es}-p_{amb} \leq p_{es,lin} \\ 0 & p_{es}-p_{amb} < 0 \end{cases} \tag{2.21}$$

$$p_{es} = \frac{p_{amb}\sqrt{\frac{p_{es,lin}}{H_{es}T_{es}}} + \sqrt{p_{es,lin}}\left(W_t + W_{wg}\right)}{\sqrt{\frac{p_{es,old}}{H_{es}T_{es}}}} \tag{2.22}$$

$$\Pi_t = \frac{p_t}{p_{em}} \tag{2.23}$$

2.2 Reduction of one control volume

Firstly one control volume at the time in the original model is replaced by a modified component. This is to make the model less stiff and thereby require a lower sample frequency.

2.2.1 Initial conditions

The states in the model are set to an initial value to get the simulation started. The initial values used throughout the entire thesis are given in table 2.1. When the states in the compressor are replaced by statical expressions, a sample and hold block is used for W_{ic}. The initial value for the mass-flow is set to 0.04915 kg/s.

Table 2.1: Initial values of the states in the model. The pressures are given in Pascal, the temperatures in Kelvin and the the rotation speed of the turbo charger in radians per second.

State	Initial value
p_{af}	99850
T_{af}	298
p_{comp}	169200
T_{comp}	374.5
p_{ic}	167300
T_{ic}	309.3
p_{im}	133700
T_{im}	309.3
p_{em}	154100
T_{em}	1100
p_{es}	109000
T_{es}	1040
ω_{TC}	11160

2.2.2 Results from simulations

In the simulations different inputs to the model are used. There are three different settings in the input signal to the throttle in the model, see figure 2.2. The other inputs to the model are set to fixed values accordingly to table 2.2. In table 2.3, the simulation results after the modifications in the model is shown. As seen in the table there are in general no large differences in sample frequency in the modified models compared to the original. One exception is when the states in the intercooler are reduced and the required sample frequency is almost doubled.

Analyzing the results, it is possible to state that there is not one single component that limits the sample frequency. Though, the best configuration of the model seems to be when the air filter is removed. The sample frequency is lowest of the configurations simulated and the errors are small compared to the other models. Figure 2.3 shows the mass-flows to the cylinders for the original model and the model with the modified air-filter. Using the modified model for the air-filter, the sample frequency is decreased by 50 Hz to 440 Hz compared to the original model. This is still a far too high frequency to achieve a stable and accurate model.

Table 2.2: Inputs to the model except throttle angle

Variable	Value
Engine speed [rpm]	2000
u_{wg}	0
λ	1
p_{amb} [Pa]	101300
T_{amb} [K]	298

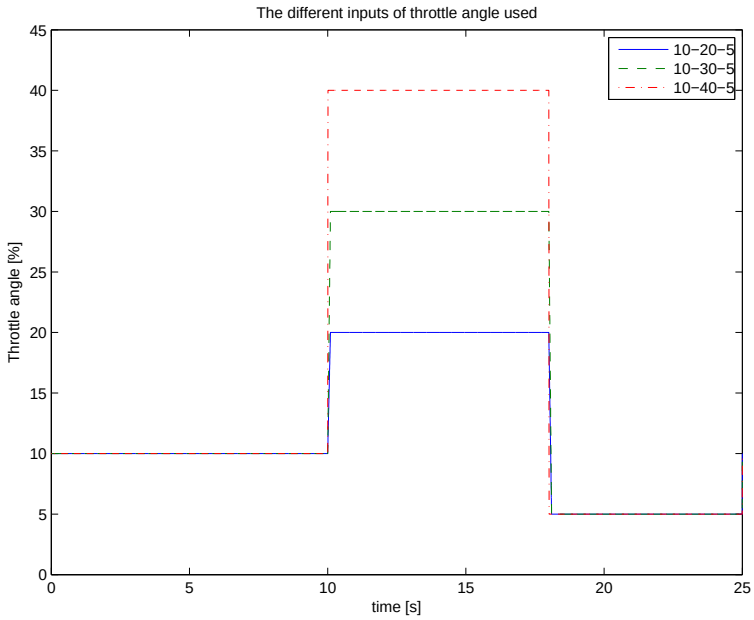

Figure 2.2: Shows the input signal of the throttle angle. There are three different inputs used in the thesis.

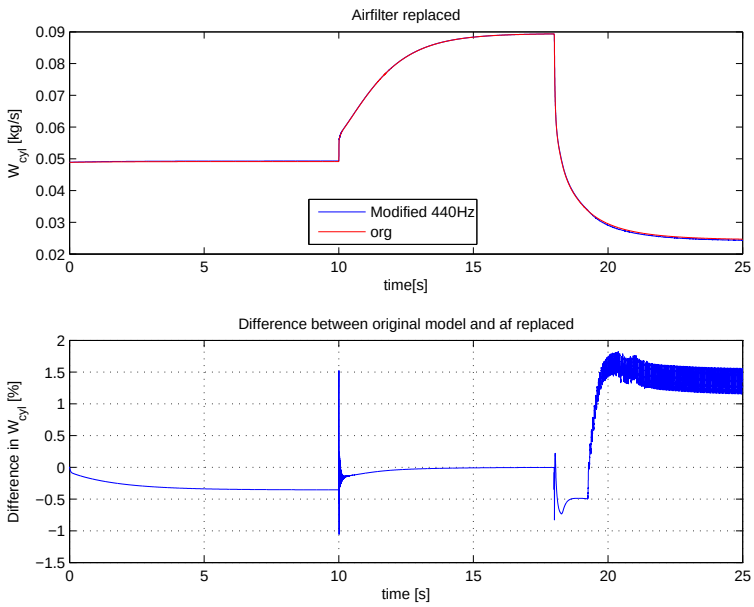

Figure 2.3: The mass-flow through the cylinders in the original model and the model with modified air-filter. The difference between the models is relatively small.

Table 2.3: Shows at what frequency the model is stable for different configurations of the model. The throttle angle used is 10_40_5 (see figure 2.2) and the solver used is an explicit Euler. An *X* indicates that the actual state is reduced.

States Replaced													$e_{I,m}$	$e_{I,s}$	$e_{I,t}$	f	$\tilde{e}_t$	$\overline{e_s}$	Nbr
p_{af}	T_{af}	p_c	T_c	p_{ic}	T_{ic}	p_{im}	T_{im}	p_{em}	T_{em}	p_{es}	T_{es}	ω_{TC}							
													-	0.20	0.20	490	5.28	0.98	1
X	X												0.32	0.17	0.31	440	1.82	0.45	2
		X	X										0.57	0.60	1.07	480	5.15	0.84	3
				X	X								1.33	0.42	1.31	970	7.23	0.70	4
							X						1.04	0.21	1.14	500	4.85	0.96	5
									X				0.16	0.21	0.24	490	5.01	0.97	6
										X	X		0.04	0.20	0.19	490	5.25	0.98	7

Table 2.4: Shows at what frequency the model is stable and accurate for different configurations of the model. The throttle angle used is 10_40_5 (see figure 2.2). The solver used is explicit Euler. An *X* indicates that the actual state is reduced.

States Replaced													$e_{I,m}$	$e_{I,s}$	$e_{I,t}$	f	$\tilde{e}_t$	$\overline{e_s}$	Nbr
p_{af}	T_{af}	p_c	T_c	p_{ic}	T_{ic}	p_{im}	T_{im}	p_{em}	T_{em}	p_{es}	T_{es}	ω_{TC}							
X	X	X	X										0.47	0.38	0.73	450	4.40	0.43	1
X	X			X	X								1.53	0.28	1.56	560	6.24	0.55	2
		X	X				X						2.11	0.46	2.29	430	7.98	0.70	3
		X	X							X	X		0.53	0.33	0.84	510	5.06	0.51	4
X	X	X	X							X	X		0.42	0.38	0.68	450	4.31	0.44	5
X	X	X	X				X			X	X		1.50	0.42	1.72	360	4.63	0.65	6
X	X	X	X				X		X	X	X		1.60	0.43	1.85	360	4.90	0.65	7
X	X	X	X		X		X		X	X	X		-	-	-	-	-	-	8
X	X			X	X		X			X	X		-	-	-	-	-	-	9

2.3 Reduction of more than one control volume

By replacing more than one of the components in the original MVEM, it is possible to reduce the sample frequency further. The results from different configurations where the model has been modified, are shown in table 2.4. The equations used to calculate the pressure in each component are the same as mentioned in chapter 2.1. The only difference is that in some cases, the pressures and temperatures used in the equation are not states any more, but instead they are calculated by statical expressions. This could lead to algebraic loops that have to be taken care of and is solved by using delay blocks that are given an initial value. This has impact on the results of the simulations since there is a delay of one sample in the signal using this block.

By analyzing the results from the simulations of the models where more than one component is modified, some conclusions can be made. The temperature in the intake manifold seems to have relatively strong impact on the sample frequency. Also the air-filter and compressor seem to be important for the sample frequency. The importance of including T_{em} as a state in the model seems to be negligible. Comparing simulation setups 6 and 7 in table 2.4 shows that the sample frequency is unchanged and the errors are almost the same for the two models.

The errors induced by the model modifications seem to be largest in the model containing the modified intake manifold. One explanation for this is that when there is a sudden change in the throttle position, T_{im} changes rapidly due to the change in pressure. When replacing the state of the temperature with a static expression this dynamics is not handled in the model any more.

The impact of modifing both the intercooler and the exhaust system is tremendous compared to only reduce the states in the intercooler, see simulation 2 in the table and simulation setup 4 in table 2.3. The sample frequency is almost halved. The difference between reducing the intercooler compared to the compressor is though more than 100 Hz (compare simulation setups 1 and 2).

In simulation 8 there are too many algebraic loops for Simulink to solve. When sample delay blocks are used to break the loops, the simulation does not become stable. Simulation setup 9, where for instance the states in the intercooler are removed the simulation is not stable even at 2000 Hz. The problem occurs after 10 seconds in combination with the step that opens the throttle.

To summarize, the most promising model configuration seems to be either number 6 or 7. Both requires a frequency of 360 Hz to achieve the level of accuracy demanded in section 1.3. In figure 2.4 the original model is compared to the model where the air-filter, compressor, inlet manifold and exhaust system are replaced by modified components (simulation 6 in table 2.4).

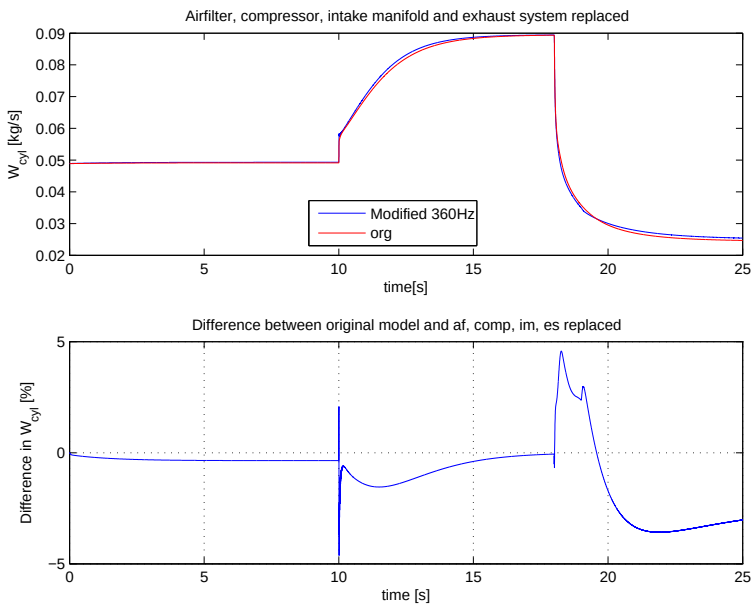

Figure 2.4: The mass-flow to the cylinders when the air filter, compressor, intake manifold and exhaust system are modified.

Chapter 3

Change Linear Regions

By reducing the number of states in the model it is possible to reduce the sample frequency to 360 Hz. Since the goal of this thesis work is to achieve a sample frequency of 80 Hz, further work has to be done. One way to go is to investigate if the size of the linear regions have any influence on the sample frequency. This could be done by analyzing the equations used, differentiate them and find when they become large. This is not done in this study. Instead the regions in the equations used in the original model are changed and compared to the previous simulations. The linear equations are not a physical way to describe the pressure and temperature and thereby induces an error. This is a trade off between lower sample frequency and greater inaccuracy in the model.

3.1 Components using linear regions

In this chapter the equations where the linear regions are used are described. In the air filter the linear region for the mass-flow is not used to calculate the pressure. The reason for this is simply that the stability of the model is worse when the linear region is implemented.

Intercooler If $p_{comp} - p_{ic} \leq p_{ic,lin}$, the linear region is used in the original model. The reason is that the derivative of W_{ic} is large for small differences in the pressures, which results in instabilities in the model.

Throttle To derive an expression for the pressure after the intercooler and intake manifold, the air mass-flow through the throttle is included. The Ψ-function, see equation 2.15, is a part of this function. When the function is differentiated with respect to Π, the square root in the numerator becomes a part of the denominator. When Π is close to 1, the magnitude of the derivate becomes large. This is the reason to use the linear regions in the original model. The Ψ-function is plotted in figure 2.1 for different linear regions. The linear region is used when $\Pi \geq \Pi_{lin}$.

The same equation for Ψ is used in the wastegate restriction. Since the same parameter is used in both components, the range of the linear region in the wastegate is changed when it is changed in the throttle. This may of course affect the stability and accuracy in the model.

Exhaust system The same basic equation for the mass-flow is used in this restriction as in the one for the intercooler. In this case the linear region is used if $p_{es} - p_{amb} \leq p_{es,lin}$.

3.2 Results

Four of the models designed in chapter 2.3 are used in this chapter. The only difference is that the linear regions are changed. The same measures of the error in the models are used as in chapter 2. The first row in the tables are the configurations used in the original models. The method for changing the linear regions is of trial and error type. It is only possible to reach a certain limit in the sample frequency by changing the linear regions. After that limit it does not matter how much the parameters are changed. Instead there are other dynamics in the model that limit the step size in the simulations. This limit is achieved in all three models in this chapter. The throttle angle used is 10_40_5 in all simulations.

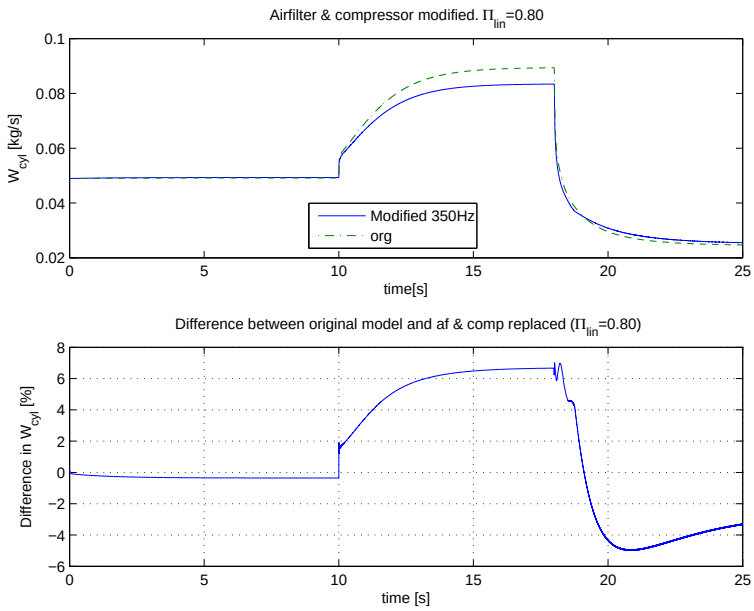

Figure 3.1: The mass-flow to the cylinders in the configuration described in simulation 4 in table 3.1.

3.2.1 Air-filter and compressor modified

The results from the different linear regions are shown in table 3.1. The model used has no states in the air-filter and the compressor.

Table 3.1: Shows at what frequency the model is stable for different ranges in the linear regions. The components that are changed compared to the original model are the air filter and compressor.

Π_{lin}	$p_{ic,lin}$	$p_{es,lin}$	$e_{I,m}$	$e_{I,s}$	$e_{I,t}$	f	$\tilde{e}_t$	$\overline{e_s}$	Nbr
0.90	800	100	0.47	0.38	0.73	450	4.40	0.43	1
0.90	1200	100	0.44	0.40	0.72	450	4.11	0.34	2
0.85	1200	100	2.17	0.33	2.40	390	5.35	0.61	3
0.80	1200	100	3.96	0.26	4.13	350	6.99	0.98	4
0.85	2000	100	2.15	0.35	2.44	390	5.24	0.46	5
0.80	2000	100	3.98	0.68	4.55	350	6.99	0.81	6

The sample frequency is reduced from 450 Hz to 350 Hz by changing the limits in the linear regions, though there are errors induced by doing so. The model error increases when Π_{lin} decreases. In simulations 4 and 6 where Π_{lin} is 0.80, the demand on accuracy of the model is no longer fulfilled, since $e_{I,t}$ is greater than 3%. A plot for W_{cyl} is shown in figure 3.1 representing the result from simulation , where Π_{lin} is 0.80 and $p_{ic,lin}$ is 1200 Pa.

The influence of the size of $p_{ic,lin}$ is negligible. The same is for $p_{es,lin}$ since the difference between the ambient pressure and p_{es} is much larger than $p_{es,lin}$ used in the simulations above. Therefore no large derivatives occurs in the model anyway.

Since both simulations that are simulated at 350 Hz not fulfill the accuracy demands, the fastest model that is approved is sampled at 390 Hz.

3.2.2 Air-filter, compressor and exhaust system modified

An alternative model to the one presented in chapter 3.2.1 is created, where also the states in the exhaust system are replaced by static equations. The result from the simulations using this model is presented in table 3.2.

The results using this configuration are very similar to the configuration where the states in the exhaust system still were part of the model. The conclusion of this is that the impact of the dynamics in the exhaust system is

Table 3.2: Shows at what frequency the model is stable for different settings in the linear ranges. The components that are changed compared to the original model are the air filter, compressor and exhaust system.

Π_{lin}	$p_{ic,lin}$	$p_{es,lin}$	$e_{I,m}$	$e_{I,s}$	$e_{I,t}$	f	$\tilde{e}_t$	$\overline{e_s}$	Nbr
0.90	800	100	0.42	0.38	0.68	450	4.31	0.44	1
0.90	1200	100	0.38	0.40	0.66	450	3.92	0.66	2
0.85	1200	100	2.12	0.35	2.38	390	5.49	0.62	3
0.85	2000	100	2.14	0.33	2.41	390	5.08	0.48	4

negligible. This is valid for the error in the model, but also for the frequency required for stability and accuracy in the model.

3.2.3 Air-filter, compressor, intake manifold and exhaust system modified

In this section the model that required lowest sample frequency when the states were reduced in chapter 2 is used. The results are shown in table 3.3. As seen, the impact of the linear regions are small on the sample frequency. The same trend as in previous model can be seen in this model. The frequency required to achieve an accurate simulation is dependent on Π_{lin}, but so are also the errors. The gain of using Π_{lin} is only 10 Hz with this configuration of the model compared to 60 Hz using the model where the air-filter, compressor and exhaust system are replaced.

Table 3.3: Shows at what frequency the model is stable for different range in the linear ranges. The components that are changed compared to the original model are the air filter, compressor, inlet manifold and exhaust system.

Π_{lin}	$p_{ic,lin}$	$p_{es,lin}$	$e_{I,m}$	$e_{I,s}$	$e_{I,t}$	f	$\tilde{e}_t$	$\overline{e_s}$	Nbr
0.90	800	100	1.50	0.42	1.72	360	4.63	0.65	1
0.90	1200	100	1.44	0.44	1.68	360	4.78	0.89	2
0.85	1200	100	2.64	0.33	2.86	350	5.45	0.99	3
0.85	2000	100	2.65	0.49	2.87	350	5.25	0.58	4

3.2.4 Air-filter, compressor, intake manifold, exhaust manifold and exhaust system modified

In chapter 2 the addition of reducing T_{em} from the model where the air-filter, compressor, inlet manifold and exhaust manifold already were replaced by statical expressions has little impact of the model. In table 3.4 the results from different linear regions are presented using the model where p_{af}, T_{af}, p_{im}, T_{im}, p_{comp}, T_{comp}, T_{im}, T_{em}, p_{es} and T_{es} are reduced. As seen there are no major differences between tables 3.4 and 3.3.

Table 3.4: Shows at what frequency the model is stable for different range in the linear ranges. The components that are changed compared to the original model are the air filter, compressor, inlet manifold, exhaust manifold and exhaust system.

Π_{lin}	$p_{ic,lin}$	$p_{es,lin}$	$e_{I,m}$	$e_{I,s}$	$e_{I,t}$	f	$\tilde{e}_t$	$\overline{e_s}$	Nbr
0.90	800	100	1.60	0.43	1.85	360	4.90	0.65	1
0.90	1200	100	1.53	0.41	1.86	370	4.14	0.80	2
0.85	1200	100	2.69	0.35	2.91	350	5.83	0.98	3
0.85	2000	100	2.65	0.49	2.87	350	5.25	0.58	4

Chapter 4

Local Differential solver

In this chapter local solvers are introduced in the model. The purpose of this is to solve parts of the model with smaller time steps in order to achieve a stable model at lower global sample frequency. The advantage of doing so is that it would take too much computational time to solve the entire model in real time with the high sample frequency.

4.1 Solvers used

Instead of using a restriction and a control volume for a component, the differential equations for the pressure and temperature are solved locally, see equations 1.2 and 1.3. To be able to solve the equations, different solver methods are introduced. The objective of this is to decrease the size of the steps in the solver in a small part of the model. If this is done on the component with the fastest dynamics in the model, the overall sample frequency can be reduced. Four different local solvers are used in this investigation. Three are implemented from scratch and one is a standard solver in Matlab. The input signals to the local solver are unchanged during each global time step.

4.1.1 Euler

This solver uses explicit Euler to solve the equations. In the model the step size in the local solver is set to be one fifth of the global step size. This solver is called *Euler* in this thesis.

4.1.2 Euler using Richardsson extrapolation

To increase the accuracy in the solver, Richardsson extrapolation [3] is used. The approach for this solver is to first simulate the values for the pressure and temperature using an ordinary Euler. This is done for two different step sizes. In this case the global step size respectively half the global step size. The difference between the results using the two different step sizes are used to give a better estimation of the actual values, see equation 4.1. This method results in that the error induced by the solver is proportional to h^2 instead of h, that is the case for explicit Euler. In this chapter this solver is called *Euler2* since the error is decreasing quadratically to the step size.

$$y_{extrapolated}(x) = y\left(x, \frac{h}{2}\right) + \frac{y\left(x, \frac{h}{2}\right) - y\left(x, h\right)}{1} \tag{4.1}$$

4.1.3 Euler using repeated Richardsson extrapolation

By using the Richardsson extrapolation one more time the accuracy of the solver increases. To be able to do this a calculation of the pressure and temperature have to be carried out at higher sample frequency. There are four points that are calculated in the local solver for every global step. A similar calculation that are carried out in equation 4.1 are made. The result from the previous extrapolation (explained in chapter 4.1.2) are reused in this calculation.

The difference between the pressure and temperature calculated can be used to estimate the accuracy of the solver. This can therefore be used to implement a solver that changes how many repeated extrapolations that should be calculated. Though, in this solver two extrapolations are allways calculated. A more accurate model should not be needed since the error of this solver is proportional to h^4. The solver is referred to as *Euler4*.

4.2 Local solver for the Intercooler

The model that is used has modified components in the airfilter, compressor, intake manifold and exhaust system. The local solver calculates p_{ic} and T_{ic}. The results from the simulations using this configuration for different local solvers are given in table 4.1. In the simulations Π_{lin}=0.85 and $p_{ic,lin}$=1200 Pa are used as linear regions. In simulation 1, no local solver is used and the simulation is the same as in chapter 3.2.3. As seen in the table, the sample frequency is significantly decreased using three of the local solvers. The reason for the bad performance using Euler2 is unknown. It should be less accurate than for example Euler4, but it is interesting that an ordinary Euler shows better performance.

In table 4.1 a new error, $e_{I,ml}$, is used. The error represents the error induced by using a local solver instead of the restriction and control volume. $e_{I,ml}$ is calculated in the same way as $e_{I,m}$ (see equation 1.6). The only difference is that the original model is replaced by the model with modified linear regions. The models compared are solved with the implicit solver *ODE15s*.

There is no great difference between the models using Euler, Euler4 or the standard solver in Matlab ODE15s. The last solver is an implicit solver. The major difference is the time it takes to simulate one driving cycle, represented as t in the table. It takes more than 10 times as long time to simulate the model when the intercooler is solved by ODE15s instead of Euler. Though the result is roughly the same.

Table 4.1: Local solver for the temperature and pressure in the intercooler. The states that is removed are $p_{af}, Taf, p_{comp}, T_{comp}, T_{im}, p_{es}$ and T_{es}. The global solver is explicit Euler.

Local Solver	f	$e_{I,m}$	$e_{I,s}$	e_{I,m_l}	$e_{I,t}$	$\overline{e}_s$	$\tilde{e}_t$	t
-	350	2.65	0.33	-	2.86	0.99	5.45	7.65
Euler	200	2.65	0.87	3.12	2.54	0.39	6.72	13.04
Euler2	320	2.40	0.61	3.38	2.00	0.84	7.05	20.14
Euler4	200	2.76	1.02	3.00	2.86	0.60	7.24	24.35
ODE15s	200	2.61	0.90	3.35	2.19	0.34	7.34	161.10

4.2.1 Different global solvers

So far in this thesis explicit Euler has been used as the global solver. When using the Simulink solver ODE5 as the global solver and using Euler in the local solver for the intercooler, the required frequency is decreased from 200 Hz to 170 Hz. ODE5 is a solver called Dormand-Prince that is a Runge-Kutta solver for the differential equations.

4.2.2 Different throttle angles

The same inputs to the model have been used throughout the whole thesis. The throttle angle used are first 10%, then 40% and finally 5% (shown in figure 2.2). During highway cruising the throttle angle might be in the range 10 to 15% open and during full acceleration about 40%. When the throttle is open the dynamics in the throttle is fast since the air rushes from the intercooler to the intake manifold with little resistance.

When using the throttle input that has a maximum throttle angle of 30% the frequency required to achieve a stable and accurate model according to the demands set in chapter 1.3 are 150 Hz. The local solver for the intercooler is Euler4 and the linear regions are the same as in table 4.1. The sample frequency is reduced by 50 Hz when the maximum throttle angle is decreased from 40% to 30%. When the maximum throttle angle is further reduced to 20% there is no change in the required sample frequency.

Chapter 5

Observer

The lowest frequency achieved using the modified MVEM is 200 Hz (see section 4.2). One reason for the high frequency is the dynamics over the throttle, when the throttle angle is large. This could be handled by using a different method to calculate the pressure and temperature in the intake manifold when the throttle is open. These states are used to estimate W_{cyl}, that is the most important variable to estimate correctly.

In this chapter, a modified throttle equation when the throttle is open, is implemented. Instead of using the modified expression in the entire MVEM, three less extensive models are implemented. The objective is to estimate W_{cyl} accurately with the models, using the available sensors in the vehicle. At the same time, the sample frequency should be decreased. The inputs to the new models are, except the input signals given in table 2.2, also pressures and temperatures in the intercooler, intake manifold and the exhaust system. The inputs to the models that are temperatures and pressures, will in a real-time application be measured by sensors. Therefore the three models are observers.

There are three different models compared. The first model uses the volumetric efficiency and thereby estimate W_{cyl}. The other models use the throttle equation in combination with the volumetric efficiency. When the throttle is open and the pressure drop is small, which results in fast dynamics, only η_{vol} is used to estimate W_{cyl}.

5.1 Volumetric efficiency

This first observer estimates W_{cyl} accordingly to equation 5.1 [2]. A model for the volumetric efficiency has to be chosen to estimate the mass-flow. In this chapter the same model is used as in the original MVEM and is presented in equation 5.2. The masked block used in the observer is shown in figure 5.1

$$W_{cyl} = \eta_{vol} \frac{V_d N p_{im}}{n_r R T_{im}} \tag{5.1}$$

$$\eta_{vol} = C_1 \frac{r_c - \left(\frac{p_{em}}{p_{im}}\right)^{\frac{1}{\gamma}}}{r_c - 1} \cdot \frac{1}{1 + \frac{1}{\lambda (A/F)_s}} \cdot \frac{T_{im}}{T_{im} - C_2 \left(\frac{1}{\lambda} - 1\right)} \tag{5.2}$$

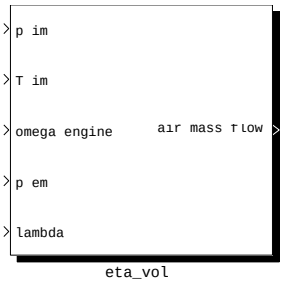

Figure 5.1: Masked block for the observer including the volumetric efficiency.

5.2 $\dot{p}_{im}$ integrated

This observer uses measured values for $p_{ic}, T_{ic}, p_{im}, T_{im}$ and p_{em}. There are two different ways of estimating the mass-flow to the cylinder in this observer.

- The first method includes the throttle equation to estimate W_{at}. The difference between W_{at} and the previous value of W_{cyl} is used to estimate $\dot{p}_{im}$, that is integrated to achieve the pressure in the intake manifold. The calculated p_{im} is then used in the calculation of η_{vol}, that is used to estimate W_{cyl}. The measured p_{im} is therefore not used in the estimation of the mass-flow in this method.
- The second way to calculate the mass-flow to the cylinders is to use the volumetric efficiency as in section 5.1. Both p_{im} and T_{im} that are used to calculate η_{vol}, are measured by sensors in this case.

The advantage of using the first method for estimating W_{cyl}, is that the sensor that measures p_{im} no longer is used. Generally p_{im} fluctuates more than for example p_{ic}. In order to achieve a mass-flow that does not fluctuate, a low-pass filter is used on the pressure signal. This filter needs a larger time constant if the signal is more fluctuating, with the result that the accuracy during transients is worse. The time constant should preferably be dependent on the frequency of the pulsations, that is dependent on the engine speed.

The advantage using the second method is that the throttle equation is not used any longer and the dynamics is reduced. Since this dynamics is fastest when the difference between p_{ic} and p_{im} is small, only the volumetric efficiency is used in these cases. When the difference between the pressures is greater than a limit, a combination of the two methods are used.The pressure ratio over the throttle, Π_{th} is used instead of the absolute difference in the pressures. The weighting functions for the two methods to estimate W_{cyl} are given in figure 5.2. The sum of the functions should of course always be unity. Using a combination of the two methods described above, results in that a combination of different pressure sensors are used.

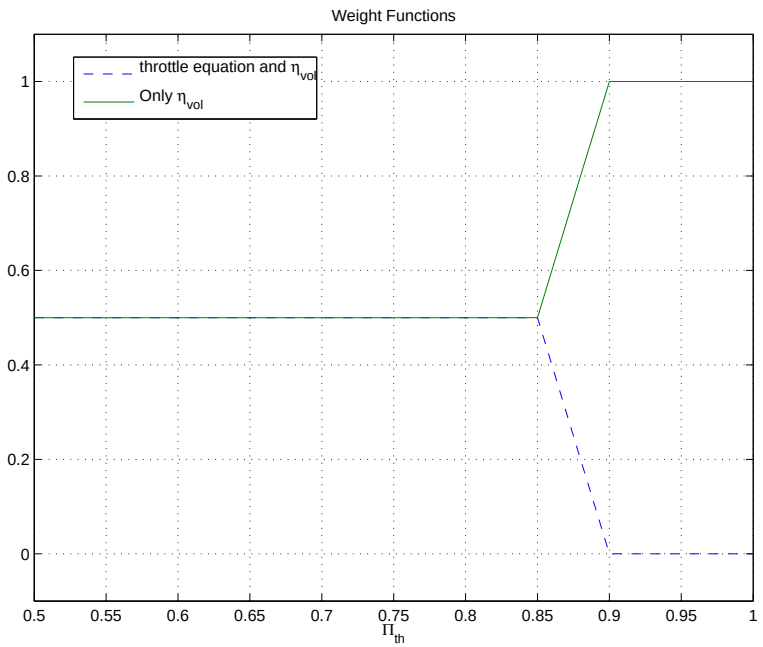

Figure 5.2: The weighting functions for the different methods of estimating W_{cyl}.

5.3 $\dot{W}_{cyl}$ integrated

This observer is similar to the observer described in section 5.2, as it calculates W_{cyl} in two different ways. The previous observer estimates W_{cyl} in the first method by calculate $\dot{p}_{im}$ and integrate it. In this observer, $\dot{W}_{cyl}$ is instead estimated and integrated. The measured p_{im} is used in this calculation, but also p_{ic}, T_{ic}, T_{im} and p_{em}.

The expression used, is derived by differentiate equation 5.1 and assuming that η_{vol}, T_{im} and the engine speed are constant in the actual operating point. Using the expression for 5.3, the expression shown in equation 5.4 is found.

The second method used includes no throttle equation and is exactly the same method as used in the previous observer. The weighting functions used to calculate the overall W_{cyl}, is the same as the previous observer and is given in figure 5.2.

$$\dot{p}_{im} = \frac{RT_{im}}{V_{im}} \left(W_{at} - W_{cyl}\right) \tag{5.3}$$

$$\frac{d}{dt}W_{cyl} = \eta_{vol}\frac{V_d N}{n_r RT_{im}}\dot{p}_{im} = \eta_{vol}\frac{V_d N}{V_{im} n_r} \left(W_{at} - W_{cyl}\right) \tag{5.4}$$

5.4 Basis for comparison

Preferably the observers designed would be compared to measurements. This is difficult since it is difficult to measure the air mass-flow to the cylinders. It would be possible to do this in steady state and use the air mass-flow sensor that is located upstream close to the throttle. The disadvantage of this method is that it is the accuracy during transients that is of highest interest. Therefore the original MVEM is used to produce inputs to the observers, but also to simulate the actual mass-flow to the cylinders. One disadvantage of this is that the input signals to the observers are free from noise and pulsations. Especially p_{im} has a periodic pulsation that is due to the opening and closing of the valves, that is not resolved in the MVEM. Therefore a sinusoidal signal with an amplitude of $1kPa$ is superpositioned on the p_{im} signal from the MVEM. The amplitude is in the same range as the pulsations in the measured data and the frequency is the same as the frequency of the engine. Of course there is noise on the other input signals to the models too, but this is neglected in this study.

If using the collected data for p_{im} (from the MVEM in this study), W_{cyl} would fluctuate. This is not to prefer and therefore a first order low pass filter is added to the pressure when it is used to estimate η_{vol}. The signal is low pass filtered in both calculations for W_{cyl} in the observer that is introduced in section 5.3. The observer where the change in pressure is integrated, does not use the measured value for p_{im} more than in the weighting function. Therefore no filter is needed in the sub-model.

5.5 Results

In this part of the thesis no quantitative measures of the errors in the models will be carried out. Instead plots will be presented and discussed. In this chapter the same inputs to the MVEM is used as presented in chapter 2.2, to generate the inputs to the observers. The throttle angle used is 10_40_5 as defined in figure 2.2

5.5.1 Low pass filter

Firstly the impact of different time constants on the low pass filter are investigated. The model used is the one that integrates $\dot{p}_{im}$ and the result is shown in figure 5.3. The plots are zoomed in from the simulation. The left plot represents W_{cyl} when the engine is run at steady state and at 10% throttle angle. The right of the two plots are the beginning of the transient when the throttle is closed from 40% to 5%. The result is as expected: the oscillations decrease and the accuracy during transients is lower when the time constant,τ, in the filter is increased. In the following part of this thesis, the time constant used will be 0.03 seconds. The reason for this is that most of the oscillations are removed from the signal, but it still has an acceptable accuracy during transients.

5.5.2 Different observers

There are three different models implemented as described above. In figure 5.4 the observers are compared when they are solved by an implicit solver (ode15s). The three plots in the figure originates from the same simulation. As seen in the plot on the top, the observer only including the volumetric efficiency, is more fluctuating than the other observers. The amplitude of the oscillations in the observers that include the throttle equation (described in sections 5.2 and 5.3), are approximately half the magnitude compared to the observer only based on η_{vol}. The explanation to this is not the same in the two observers. When $\dot{p}_{im}$ is integrated, the measured p_{im} is not included in the estimation of the mass-flow through the throttle. Since p_{im} is the only signal that oscillates, W_{cyl} does

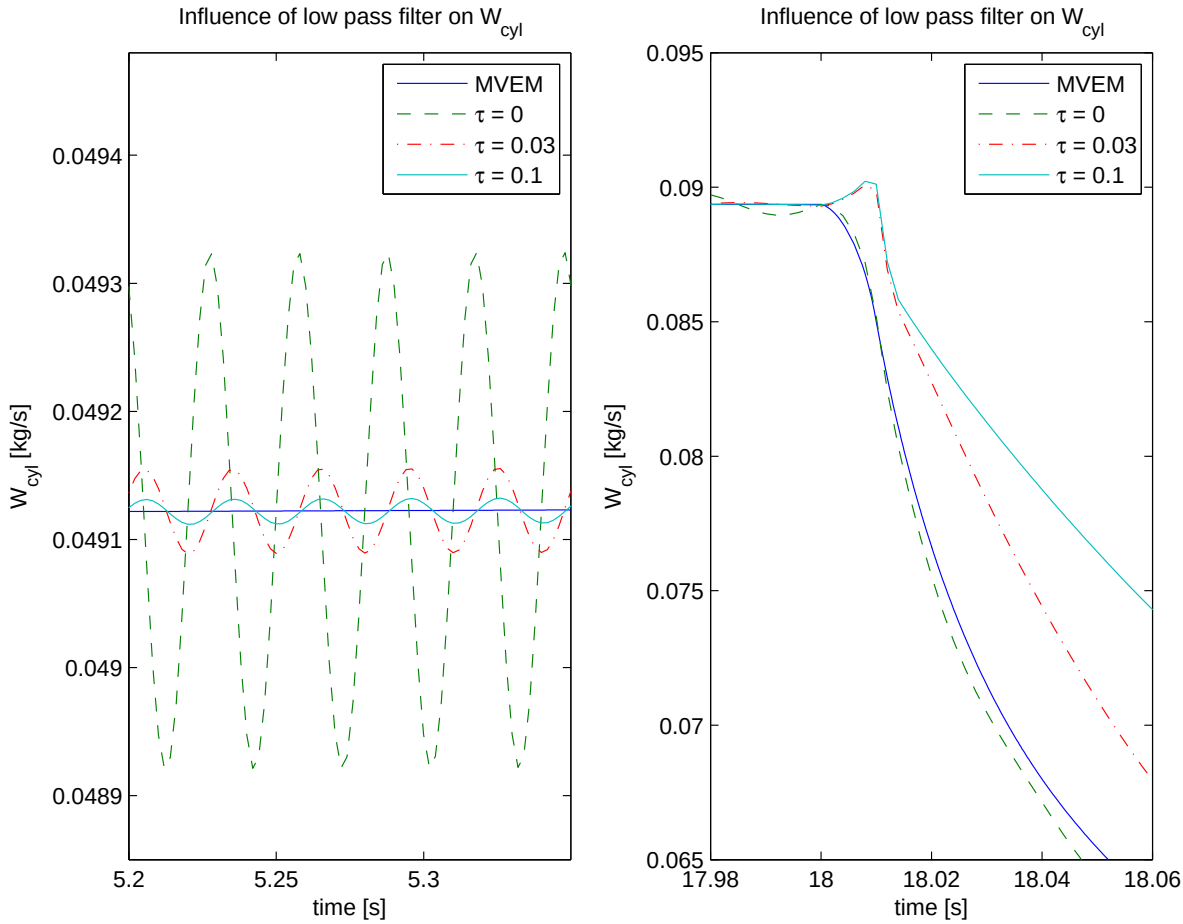

Figure 5.3: The influence on the model described in section 5.2 using a low pass filter with different time constants.

not have any oscillations from the part that is based on the throttle equation. In the region for the plot, Π_{th} is lower than 0.85 and therefore the two different ways of calculating the estimated W_{cyl} is weighted equally (see figure 5.2). Therefore, the magnitude of the oscillations is halved in this case. For the observer where $\dot{W}_{cyl}$ is integrated, the oscillations in W_{cyl}, that is estimated using the throttle equation, are marginally larger than the mass-flow estimated only using η_{vol}. The reason for the total decrease in magnitude of the oscillations in the mass-flow is that there is a phase shift of almost $180°$. This leads to that when adding the different estimations for W_{cyl}, the oscillations will counteract each other.

In the lower left plot in figure 5.4, a step in throttle angle from 10% to 40% occurs. When the estimated W_{cyl} from the three observers coincide (approximately at time 10.007 seconds), Π is higher than 0.90 and the throttle equations are not used any more. That means that all models only use the model for the volumetric efficiency. As seen in the plot, the difference is large between the MVEM and the model where $\dot{W}_{cyl}$ is integrated, in the beginning of the transient. The error is at the most in the range of 30%. The reason for this is mainly that η_{vol}, engine speed and T_{im} are assumed to be constant in this observer, though this is not the case during transients. To be able to handle this a more complex model has to be implemented.

After the transient in throttle angle from 40% to 5% (see the lower right plot), a large error in the estimated mass-flow is made in the observer that integrates $\dot{W}_{cyl}$. The reason for this is most likely the same as in the first transient (discussed above). The observer that integrates $\dot{p}_{im}$ has a faster step response than the model that only uses the volumetric efficiency. This transient is more interesting than the first transient, since Π is below 0.85 after the transient and therefore the model for the throttle is used and it is that part that differs in the models.

In figure 5.5, the solver used in the simulations is explicit Euler. The figure has the same layout as figure 5.4. The same structures can be seen using Euler as the solver as when ode15s is used. The mass-flow calculated by the MVEM is still from a simulation where the implicit solver is used. The observers called *volumetric* and $\dot{p}_{im}$

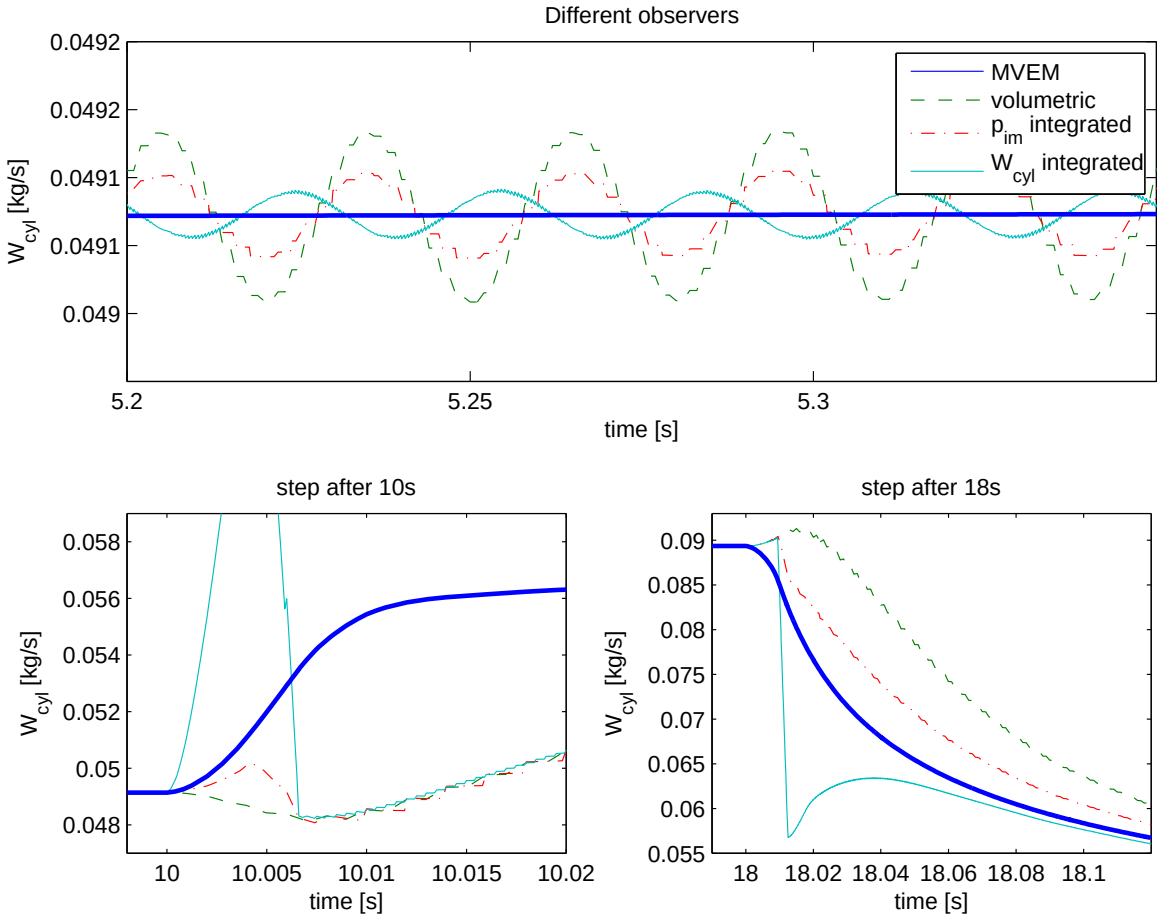

Figure 5.4: Different observers compared using the same inputs as in section 2.2 and throttle angle 10_40_5. The thicker line represents W_{cyl} from the MVEM. The time constant in the low pass filters is set to 0.03 seconds and the solver used is ode15s. In the lower left plot, W_{cyl} peaks at 0.067 kg/s in the model where $\dot{W}_{cyl}$ is integrated.

integrated in the figure has a sample frequency of 80 Hz. It is possible to use a lower frequency. The disadvantage of this is that the frequency of the oscillations in the measured p_{im} are equal to the engine frequency, which is about 33 Hz in this case. As a consequence, the accuracy in the observer will be bad, no matter what model is used, if there are not enough samples during one period.

The observer that integrates the mass-flow is not stable if the sample frequency is lower than 390 Hz. The instability occurs before the first step in the throttle. What causes the instability is not investigated in this thesis.

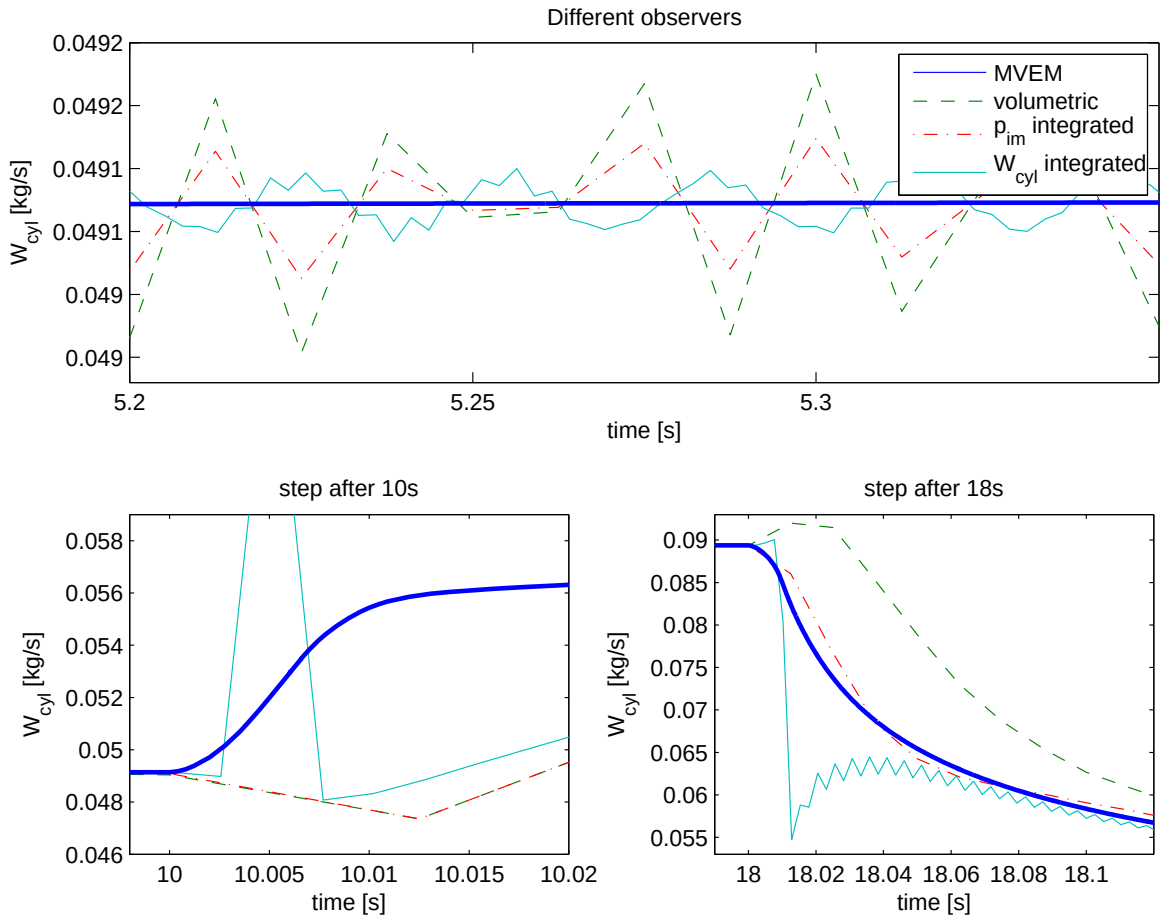

Figure 5.5: Different observers compared using the same inputs as in section 2.2 and throttle angle 10_40_5. The thicker line is W_{cyl} from the MVEM. The time constant in the pass filters are set to 0.03 seconds and the solver used is explicit Euler for the observers. The sample frequency is 80 Hz for the *volumetric* and $\dot{p}_{im}$, but 390 Hz for the third observer. In the lower left plot, W_{cyl} peaks at 0.067 kg/s in the model where $\dot{W}_{cyl}$ is integrated.

Chapter 6

Summary and Conclusions

The objective of the thesis is to increase the stability of the model. In chapter 2 the original MVEM is modified, mainly by reducing the number of states in the model. The fastest model that is investigated in the chapter, still requires a sample frequency of 360 Hz to fulfill the accuracy demands. This is a far too high frequency and higher than was expected when the thesis started.

Changing the linear regions (see chapter 3) has an impact on the accuracy that is more significant compared to removing the states. The reduction in the sample frequency by doing this modification is very small. Though, in order to decrease the sample frequency to 80 Hz, it will most likely be needed to change the linear regions. Therefore, it is of importance to understand the impact on the accuracy in the model that the changes in the regions induce.

A local solver is implemented to calculate the pressure and temperature in the intercooler. This has significant impact in the required frequency and it is decreased to 200 Hz. The disadvantage of using a local solver is that the required computational power increases. Instead it would be preferable to rewrite the expression used, for the operating points that are crucial.

The accuracy and sample frequency for stability in the different observers vary significantly. The inputs to the observers will be signals from the sensors in the vehicle. Since the inputs in the validation of the models instead are from a MVEM-simulation, no white noise and pulsations are super-positioned on the mean valued signals. Therefore it is difficult to comment on the reliability in the results presented in chapter 5.

One disadvantage using an observer of the kind that is implemented in chapter 5, is that the input signals have to be low pass filtered. This is to avoid that the estimated mass-flow through the cylinders not are fluctuating. This leads to that the response time during transients are longer, compared to using an observer based on the entire MVEM. The MVEM can handle the changes in operating points faster than the sensors react and therefore the estimated W_{cyl} is more accurate during transients. This is not possible to do in the same extent, using the smaller models in the observers.

Chapter 7

Future Work

Different proposals for further investigations are given below.

- It would be interesting to implement an alternative model for the flow through the throttle in the MVEM, instead of using one of the observers implemented in chapter 5. This model should be active when the throttle angle is large and the pressure ratio over the throttle is close to unity. This is the way the observers are implemented. The purpose of implement this in the MVEM, is that the sample frequency in the model hopefully will decrease. At the same time, the accuracy during transients will be higher compared to the observers.

- Validate the different observers implemented in chapter 5, by using measured data. An alternative way is to implement the observers in the controller system in a vehicle and compare the estimated mass-flow to the actual mass-flow. This could for example be performed by using the λ-sensor.

- Analyze what would happen if another frequency of the pulsations on p_{im} is used instead of 33 Hz. The observer that integrates the mass-flow has a relatively low pulsation in W_{cyl}. The reason is that the pulsations in the two sub-models have a phase shift of almost 180° between each other and therefore counteract. It is not sure this will be the case when the engine is running at another speed. In worst case the pulsations will interfere constructively.

References

[1] Per Andersson. *Air Charge Estimation in Turbocharged Spark Ignition Engines*. Phd thesis 989, Department of Electrical Engineering, Linköpings Universitet, Linköping, Sweden, 2005.

[2] Lars Eriksson and Lars Nielsen. Modeling and control of internal combustion engines. Compendium, 2005.

[3] Linde Wittmeyer-Koch Lars Eldén and Hans Bruun Nielsen. *Introduction to Numerical Computation - analysis and Matlab illustrations*. Studentlitteratur, Lund, Sweden, 2004.

[4] Frank M. White. *Fluid Mechanics*. McGraw-Hill, 5 edition, 2003.

Nomenclature

Variables and parameters

Symbol	Description	unit
p	Pressure	Pa
T	Temperature	K
V	Volume	m^3
R	Ideal gas constant	$\frac{J}{mole \cdot K}$
W	Mass-flow	$\frac{kg}{s}$
m	Mass	kg
c_v	Specific heat at constant volume	$\frac{J}{kg \cdot K}$
$\dot{Q}$	Heat-flow	W
H	Pressure head-loss parameter	$\frac{Pa^2 s^2}{K \cdot kg^2}$
D	Diameter	m
A_{eff}	Effective area in the throttle	m^2
f	Frequency	$[Hz]$
h	Step size	$[s]$
V_d	Cylinder volume	$[m^3]$
r_c	Compression ratio	$-$
ω	angular speed	$\frac{rad}{s}$
Π	Pressure ratio	$-$
η_{vol}	volumetric efficiency	$-$
$MVEM$	Mean Value Engine Modeling	

Subscripts

Subscript	Location
af	Air-filter
$comp$	Compressor
ic	Intercooler
im	Intake manifold
em	Exhaust manifold
es	Exhaust system
amb	Ambient
TC	Turbo charger
us	Upstream
ds	Downstream
r	Restriction
lin	Linear
wg	Wastegate
t	turbine
at	throttle